

## Response of a Spherical Bubble Cloud

The corresponding shielding effects during forced excitation are illustrated in figure 1, which shows the distribution of the amplitude of bubble radius oscillation,  $|\varphi|$ , within the cloud at various excitation frequencies,  $\omega$ . Note that, while the entire cloud responds in a fairly uniform manner for  $\omega < \omega_n$ , only a surface layer of bubbles exhibits significant response when  $\omega > \omega_n$ . In the latter case the entire core of the cloud is essentially shielded by the outer layer.

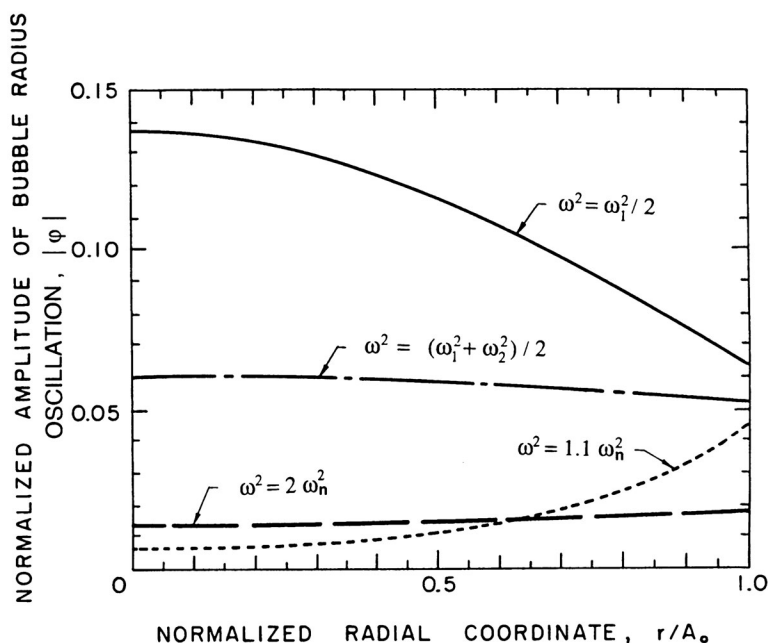


Figure 1: The distribution of bubble radius oscillation amplitudes,  $|\varphi|$ , within a cloud subjected to forced excitation at various frequencies,  $\omega$ , as indicated (for the case of  $\alpha_o(1 - \alpha_o)A_o^2/R_o^2 = 0.822$ ). From d'Agostino and Brennen (1989).

The variations in the response at different frequencies are shown in more detail in figure 2, in which the amplitude at the cloud surface,  $|\varphi(A_o, t)|$ , is presented as a function of  $\omega$ . The solid line corresponds to the above analysis, that did not include any bubble damping. Consequently, there are asymptotes to infinity at each of the cloud natural frequencies; for clarity we have omitted the numerous asymptotes that occur just below the bubble natural frequency,  $\omega_n$ . Also shown in this figure are the corresponding results when a reasonable estimate of the damping is included in the analysis (d'Agostino and Brennen 1989). The attenuation due to the damping is much greater at the higher frequencies so that, when damping is included (figure 2), the dominant feature of the response is the lowest natural frequency of the cloud. The response at the bubble natural frequency becomes much less significant.

The effect of varying the parameter,  $\alpha_o(1 - \alpha_o)A_o^2/R_o^2$ , is shown in figure 3. Note that increasing the void fraction causes a reduction in both the amplitude and frequency of the dominant response at the lowest natural frequency of the cloud. d'Agostino and Brennen (1988) have also calculated the acoustical absorption and scattering cross-sections of the cloud that this analysis implies. Not surprisingly, the dominant peaks in the cross-sections occur at the lowest cloud natural frequency.

It is important to emphasize that the analysis presented above is purely linear and that there are likely to be very significant nonlinear effects that may have a major effect on the dynamics and acoustics of

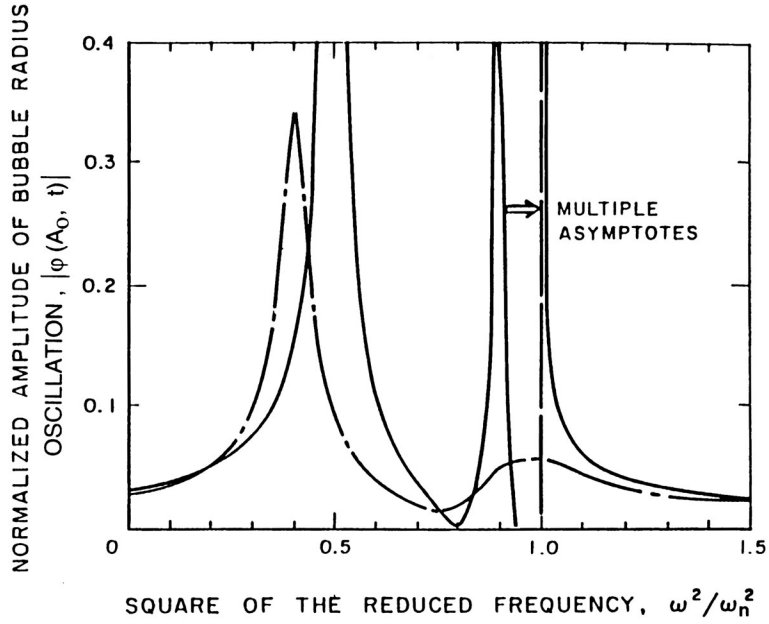


Figure 2: The amplitude of the bubble radius oscillation at the cloud surface,  $|\varphi(A_o, t)|$ , as a function of frequency (for the case of  $\alpha_o(1 - \alpha_o)A_o^2/R_o^2 = 0.822$ ). Solid line is without damping; broken line includes damping. From d'Agostino and Brennen (1989).

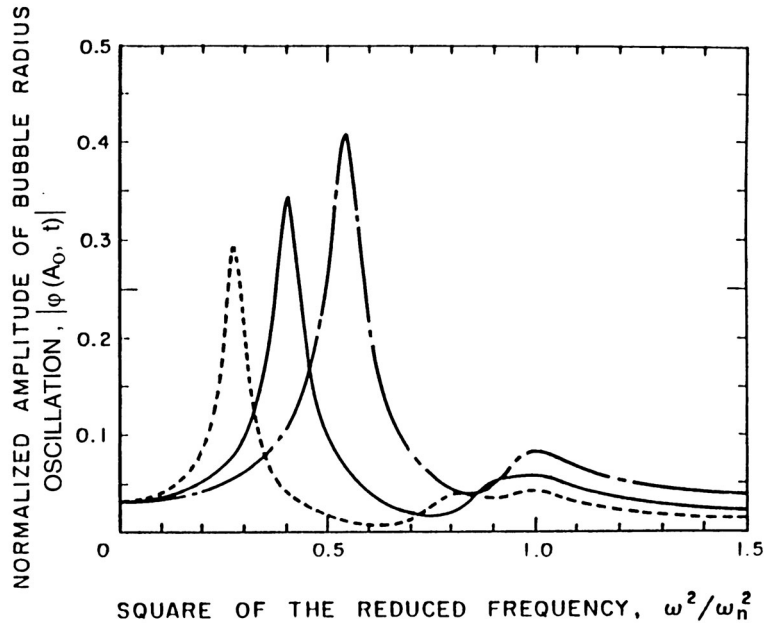


Figure 3: The amplitude of the bubble radius oscillation at the cloud surface,  $|\varphi(A_o, t)|$ , as a function of frequency for damped oscillations at three values of  $\alpha_o(1 - \alpha_o)A_o^2/R_o^2$  equal to 0.822 (solid line), 0.411 (dot-dash line), and 1.65 (dashed line). From d'Agostino and Brennen (1989).

real bubble clouds. Hanson *et al.* (1981) and Mørch (1980, 1981) visualize that the collapse of a cloud of bubbles involves the formation and inward propagation of a shock wave and that the focusing of this shock at the center of the cloud creates the enhancement of the noise and damage potential associated with cloud collapse. The deformations of the individual bubbles within a collapsing cloud have been examined numerically by Chahine and Duraiswami (1992), who showed that the bubbles on the periphery of the cloud develop inwardly directed re-entrant jets.

Numerical investigations of the nonlinear dynamics of cavity clouds have been carried out by Chahine (1982), Omta (1987), and Kumar and Brennen (1991, 1992, 1993). Kumar and Brennen have obtained weakly nonlinear solutions to a number of cloud problems by retaining only the terms that are quadratic in the amplitude. One interesting phenomenon that emerges from this nonlinear analysis involves the interactions between the bubbles of different size that would commonly occur in any real cloud. The phenomenon, called *harmonic cascading* (Kumar and Brennen 1992), occurs when a relatively small number of larger bubbles begins to respond nonlinearly to some excitation. Then the higher harmonics produced will excite the much larger number of smaller bubbles at their natural frequency. The process can then be repeated to even smaller bubbles. In essence, this nonlinear effect causes a cascading of fluctuation energy to smaller bubbles and higher frequencies.

In all of the above we have focused, explicitly or implicitly, on spherical bubble clouds. Solutions of the basic equations for other, more complex geometries are not readily obtained. However, d'Agostino *et al.* (1988) have examined some of the characteristics of this class of flows past slender bodies (for example, the flow over a wavy surface). Clearly, in the absence of bubble dynamics, one would encounter two types of flow: subsonic and supersonic. Interestingly, the inclusion of bubble dynamics leads to three types of flow. At sufficiently low speeds one obtains the usual elliptic equations of subsonic flow. When the sonic speed is exceeded, the equations become hyperbolic and the flow supersonic. However, with further increase in speed, the time rate of change becomes equivalent to frequencies above the natural frequency of the bubbles. Then the equations become elliptic again and a new flow regime, termed *super-resonant*, occurs. d'Agostino *et al.* (1988) explore the consequences of this and other features of these slender body flows.